Eddy impacts on the marine biogeochemistry of the California Current System

Pierre Damien[1], Daniele Bianchi[1], Fayçal Kessouri[2], James C. McWilliams[1]

[1]University of California, Los Angeles, CA
[2]Southern California Coastal Water Research Project, Costa Mesa, CA

Key Points:

- In the California Current, subduction by submesoscale eddies near the coast and mesoscale eddies offshore reduces surface nutrients.
- In the presence of submesoscale eddies, the non-linear nature of nutrient uptake decreases primary production by up to $\sim 50\%$.
- The amplitude and sign of eddy nutrient uptake is controlled by the covariance of temperature, nutrient and phytoplankton fluctuations.

Corresponding author: Pierre Damien, pdamien@ucla.edu

Abstract

Eddies play a crucial role in shaping ocean dynamics by affecting material transport, and generating spatio-temporal heterogeneity. However, how eddies at different scales modulate biogeochemical transformation rates remains an open question. Applying a multi-scale decomposition to a numerical simulation, we investigate the respective impact of mesoscale and submesoscale eddies on nutrient transport and biogeochemical cycling in the California Current System. First, the non-linear nature of biological nutrient uptake results in a 50% reduction in primary production in the presence of eddies. Second, eddies shape the vertical transport of nutrients with a strong compensation between mesoscale and submesoscale. Third, the eddy effect on nutrient uptake is controlled by the covariance of temperature, nutrient and phytoplankton fluctuations caused by eddies. Our results shed new light on the tight interaction between non-linear fluid dynamics and ecosystem processes in realistic eddy regimes, highlighting the importance of both mesoscale and submesoscale variability.

1 Introduction

Mesoscale and submesoscale eddies are ubiquitous in the ocean, and play a central role in its dynamics. Eddies directly influence transport of momentum and material properties, and generate spatial and temporal heterogeneity in biogeochemical tracers and transformation rates (McGillicuddy, 2016; Mahadevan, 2016; Lévy et al., 2018). In contrast with the mean oceanic circulation, eddy dynamics is generally described as that occurring on time scales shorter than a few months, and spatial scales of a hundred of kilometers or less. Transport of material properties at these scales (i.e., eddy-induced fluxes) arises from the covariance of tracer and momentum fluctuations around their large-scale means (Levy & Martin, 2013). Because of the prevalence of eddies in the oceanic kinetic energy spectrum (Chelton et al., 2007), eddy fluxes often represent major contributions to momentum and material exchanges, sometimes rivaling transport by the mean circulation (McGillicuddy et al., 2003; Lévy et al., 2012).

Circulation at eddy scales affects biogeochemistry in multiple ways. In the simplest way, eddy-induced physical-biogeochemical interactions occur via two main processes: eddy transport and eddy reaction rates (Levy & Martin, 2013). These are are similar in essence, but reflect different underlying mechanisms (Goodman & Robinson, 2008). Eddy transport arises from eddy-scale correlations between fluctuations in currents and tracer concentrations. This is an advective stirring process with both vertical (Falkowski et al., 1991; Oschlies & Garcon, 1998; Benitez-Nelson et al., 2007; F. Kessouri et al., 2020) and horizontal (Lathuilière et al., 2010; Gruber et al., 2011; Gaube et al., 2014) contributions. The effects of eddy transport depend on the circulation regime and large-scale biogeochemical gradients, and remain an active field of investigation (Lévy et al., 2018).

Eddy reaction rates consist of a "rectification" of large-scale, low-frequency biogeochemical transformation rates that arises from the non-linear nature of biogeochemical interactions (which include primary production, zooplankton grazing, remineralization) in a turbulent, heterogeneous environment. As a result, biogeochemical transformation rates estimated from a "mean field approximation", i.e., estimated from properties averaged over scales greater than those of eddies, often fail to represent the biogeochemical dynamics of a turbulent ocean (Rovinsky et al., 1997; Brentnall et al., 2003). In analogy to eddy transport fluxes, a Reynolds decomposition can be applied to biogeochemical rates to separate mean from eddy contributions. This approach relies on appropriate spatial or temporal filters to separate the effects of the mean tracer distribution from fluctuations induced by eddies (Goodman & Robinson, 2008; Wallhead et al., 2008; Goodman, 2011).

Beyond theoretical and idealized studies (Brentnall et al., 2003; Goodman & Robinson, 2008; Wallhead et al., 2008), Levy and Martin (2013) showed that eddy contribu-

tions accounted for between 5 and 30% of primary production and grazing rates in an idealized, eddy-resolving simulation of the North Atlantic Ocean. Eddy effects were mostly attributed to mesoscale variability (with typical length scales of between 30 and 100 km). A somewhat weaker eddy contribution was confirmed by analysis of *in situ* and satellite observations in the same region (Martin et al., 2015), suggesting that, while non-negligible, eddy reaction rates may have only a minor impact on open-ocean biogeochemistry. However, these estimates focused mostly on mesoscale eddies, while submesoscales remained under-resolved and under-sampled. Thus, it is possible that, in region with vigorous submesoscale activity — such as intense frontal regions and upwelling systems, eddy reactions may be more important than previously appreciated.

The California Current System (CCS) is ideally suited for studies of eddy-driven physical-biogeochemical interactions. In this coastal environment, wind-driven upwelling of nutrient-rich waters fuels intense biological productivity (Carr & Kearns, 2003; Messié et al., 2009) and generates a highly energetic field of mesoscale and submesoscale eddies (Marchesiello et al., 2003; Capet et al., 2008). Baroclinic instabilities of the alongshore current (Marchesiello et al., 2003) result in a cross-shore transport of nutrients and organic material followed by subduction along the CCS fronts. This so-called "eddy quenching" process (Gruber et al., 2011) reduces productivity in the coastal band, and supplies nutrients to remote open-ocean regions (Lovecchio et al., 2018; Yamamoto et al., 2018; Frenger et al., 2018). At the submesoscale, eddies enhance both nutrient removal in the coastal region, and nutrient entrainement and re-supply to the euphotic zone offshore (F. Kessouri et al., 2020). However, the contribution of submesoscale and mesoscale eddy transports in this upwelling system remains poorly characterized, and the impact of eddies on biogeochemical reactions rates has not been quantified yet.

Here, we evaluate the role of mesoscale and submesoscale eddies on nutrient transport and uptake rates by applying a multi-scale Reynolds decomposition to output from a submesoscale-permitting model of the CCS (F. Kessouri et al., 2020; Damien et al., 2023). Our analysis provides new insights on the different routes of nutrient supply and removal in the euphotic layer, and on the scale-dependent interplay between non-linear fluid and ecosystem dynamics in a highly heterogeneous environment.

2 Methods

2.1 Physical-biogeochemical model

We use the Regional Ocean Modeling System (ROMS, (Shchepetkin & McWilliams, 2005)) coupled online to the Biogeochemical Elemental Cycling model (BEC, (Moore et al., 2004; Deutsch et al., 2021)). ROMS solves the hydrostatic primitive equations for the tree-dimensional velocity, temperature, salinity and the transport of tracers in a terrain-following coordinate system. BEC represents the biogeochemical cycles of major elements (C, N, P, O, Fe, Si) resulting from the interaction of three phytoplankton and one zooplankton group.

We analyze output from two twin simulations for the northern and southern U.S. West Coast at 1 km resolution (Damien et al., 2023), sufficient to allow emergence of submesoscale dynamics (F. Kessouri et al., 2020), obtained by dynamical downscaling of a coastwide configuration at 4 km resolution (Renault et al., 2021; Deutsch et al., 2021). Because these simulations do not include tidal forcings, the highest frequencies captured by the model only include submesoscale circulation and internal waves generated within the domain. Output consists of physical and biogeochemical variables, transport fluxes, and biogeochemical rates calculated online by the model, and is saved as daily averages.

In the model, an arbitrary biogeochemical tracer X_i obeys the conservation equation:

$$\partial_t X_i = T(X_i) + \partial_z(\kappa\, \partial_z\, X_i) + J_i(X_{j=1,\dots,J}). \tag{1}$$

The first term on the right hand side, $T(X_i) = -\nabla \cdot (\mathbf{u}\, X_i)$, represents the divergence of the advective flux, with $\mathbf{u} = (u, v, w)$ the velocity vector. It can be further decomposed into a horizontal $T_h(X_i)$ and vertical $T_v(X_i)$ component. The second term represents vertical mixing, with κ the vertical eddy diffusivity. The third term, J_i, is the sum of all biogeochemical rates that affect the tracer X_i, which in turn depend on J model state variables X_j.

We focus on the balance of nitrate (NO_3^-), the main limiting nutrient in the CCS (Deutsch et al., 2021). For this variable, the net biogeochemical reaction rate is:

$$J = J^{Uptk} + J^{Nit} + J^{Denit} \tag{2}$$

Here, J^{Uptk} is the rate of uptake by phytoplankton, J^{Nit} production by nitrification, and J^{Denit} consumption by denitrification. Note that here, J^{Uptk} is a negative rate because it removes nutrient from sea water. Therefore, it is equivalent to net primary production, but with an opposite sign, and expressed in nitrogen units. In the CCS, denitrification only occurs in the deeper parts of anoxic basins and in the sediment, and is a minor term compared to nitrification and biological uptake. Hence, when discussing water column processes, we focus primarily on nitrification and uptake. The nitrification rate, $J^{Nit} = \tau^{nit}\ NO_2^-$, is modeled as a linear function of nitrite (NO_2^-) concentration, with τ^{nit} a constant timescale. Non-linearities in nitrification arise from limitation under high irradiance in the euphotic zone, and inhibition at vanishing oxygen and nitrite concentrations (Deutsch et al., 2021). Biological uptake depends on nutrient concentrations following a Michaelis-Menten kinetics and Liebig's law of the minimum, phytoplankton biomass, and a temperature- and light-dependent growth rate (see Supporting Information T2, and Deutsch et al. (2021)). Thus, uptake is highly non-linear because of the presence of bilinear ($X_i X_j$), exponential (e^{X_i}), and hyperbolic (Michaelis-Menten) terms.

2.2 Triple decomposition of transport and biogeochemical rates

The non-linear nature of advection, nitrification, and uptake in the nitrate conservation equation (Equation 1) is at the root of eddy rectification effects that modulate the final rate of change of this tracer.

To separate the effects of mesoscale and submesoscale eddies, we apply a triple Reynolds decomposition based on two low-pass filters, $\overline{\cdot}$ and $\widetilde{\cdot}$, with respective space/time scales $\overline{(\lambda, \tau)}$ and $\widetilde{(\lambda, \tau)}$ (Capet et al., 2008). Accordingly, a model variable X_i is decomposed into mean and fluctuating mesoscale and submesoscale components as:

$$X_i = \overline{X_i} + X_i' + X_i'', \tag{3}$$

where

$$X_i' = \widetilde{X_i} - \overline{X_i} \quad \text{and} \quad X_i'' = X_i - \widetilde{X_i}. \tag{4}$$

By definition, $\overline{X_i'} = 0$ and $\widetilde{X_i''} = 0$. Here, $\overline{(\lambda, \tau)}$ and $\widetilde{(\lambda, \tau)}$, are chosen to separate mesoscale (X_i') and submesoscale (X_i'') fluctuations from a large-scale, low-frequency mean ($\overline{X_i}$) that includes the seasonal cycle. The X_i'' component represents the smallest scales and highest frequencies allowed by the model, i.e., mostly submesoscales. The choice of the filter scales is dependent on the circulation regime, and may not always perfectly separate intrinsic variability from forced motions. For example, along the U.S. West Coast, wind-driven upwelling is generally considered part of the mean seasonal variability. However, short-term wind events can generate high frequency variability in circulation that overlaps with mesoscale and submesoscale motions. In our choice of filters, we were especially careful to attribute the main upwelling signal to large-scale regional variability (i.e., the mean term $\overline{X_i}$) and not higher frequency fluctuations. To this end, we found a reasonable combination of temporal and spatial filter scales, defined as follows:

- $\overline{(\lambda, \tau)}$ = (15 km,3 months), with a centered averaging scheme,
- $\widetilde{(\lambda, \tau)}$: (5 km, 3 days), with a centered averaging scheme.

We refer the readers to Supporting Information T1 that further discusses these filters and their performance, using surface temperature and vertical velocities as an illustration.

By applying these filters to model variables, biogeochemical transformation rates can be separated into mean and eddy components. For a nonlinear reaction rate $J_i(X_j)$ with dependence on multiple variables X_j, $j = 1, ..., J$ and the transport divergence $T(X_i)$, the analogous Reynolds decomposition takes the form:

$$J = J^{mean} + J^{meso} + J^{subm} \quad \text{and} \quad T = T^{mean} + T^{meso} + T^{subm} \tag{5}$$

where the various terms are now calculated as:

$$J^{mean} = J_i(\overline{X_j}) \quad \text{and} \quad T^{mean} = T(\overline{X_i}) \tag{6}$$

$$J^{meso} = J_i(\widetilde{X_j}) - J_i(\overline{X_j}) \quad \text{and} \quad T^{meso} = T(\widetilde{X_i}) - T(\overline{X_i}) \tag{7}$$

$$J^{subm} = J_i(X_j) - J(\widetilde{X_j}) \quad \text{and} \quad T^{subm} = T(X_i) - T(\widetilde{X_i}) \tag{8}$$

By adopting the filtering approach discussed above, the three terms in Equation 5 can be respectively interpreted as the contribution to the total rate caused by the large-scale mean tracer distributions (J^{mean} and T^{mean}); the contribution caused by heterogeneity at the scale of mesoscale eddies (J^{meso} and T^{meso}); and the contribution caused by heterogeneity at submesoscales and smaller scales captured by the model (J^{subm} and T^{subm}). Specifically, the biogeochemical eddy contributions only exist as a rectification of biogeochemical rates that depend in non-linear ways on model variables. These contributions would vanish in the case of perfectly linear rates (Levy & Martin, 2013).

2.3 Amplitude and sign of the eddy rectification

Assuming high frequency fluctuations of small amplitudes relative to the mean, the low frequency and large scale advective transport (T) and biogeochemical rates (J) can be approximated by a Taylor series expansion (Levy & Martin, 2013):

$$\overline{J(X_i)} = J(\overline{X_i}) + \sum_i \frac{\partial J}{\partial X_i}\bigg|_{\overline{X_i},\overline{X_j},...} \overline{X_i'} + \frac{1}{2}\sum_{i,j} \frac{\partial^2 J}{\partial X_i \partial X_j}\bigg|_{\overline{X_i},\overline{X_j},...} \overline{X_i' X_j'} + O(\overline{X_i' X_j' X_k'}) \tag{9}$$

An equivalent Taylor expansion can be written for the advection term T, leading to a typical definition of eddy transport fluxes (Capet et al., 2008). Since the fluctuations have zero mean, the linear terms disappear. Ignoring the contribution of third-order terms, the amplitude and sign of the eddy rectified effect depend on the curvature of the functional dependencies (encapsulated by J) and eddy correlation terms between model variables ($\overline{X_i' X_j'}$):

$$\overline{J^{eddy}} \approx \frac{1}{2}\sum_{i,j} \frac{\partial^2 J}{\partial X_i \partial X_j}\bigg|_{\overline{X_i},\overline{X_j},...} \overline{X_i' X_j'} \tag{10}$$

3 Results

We find that, along the CCS coast, the balance of nitrate in the surface layer (Equation 1) reflects a near compensation of two major terms: biological uptake (J^{Uptk}), and the divergence of the vertical transport (T_v) (Figure 1). The mean component of J^{Uptk} increases towards the coast (Figure 1a), reflecting high nutrient concentrations following inputs by upwelling (Figure 1d). Both mesoscale and submesoscale contributions to J^{Uptk} are opposite in sign and partially offset the mean component. The magnitude of

the submesoscale contribution is particularly large, reaching about -34% of the mean J^{Uptk}, while the mesoscale contribution is more limited.

Supply of NO_3^- by vertical transport (i.e., the divergence of the vertical flux; Figure 1d-f) shows noisier patterns, reflecting the high variability and large magnitude of advective fluxes. However, notable patterns emerge. The most significant is the positive mean T_v (i.e., NO_3^- supply) along the coastal band caused by upwelling. The submesoscale T_v largely opposes the mean upwelling along the coast, reducing NO_3^- supply by 50 to 70%. In contrast, mesoscale T_v is weaker, and is characterized by upwelling close to the coast, and downwelling offshore, thus reinforcing the mean vertical transport.

Based on these patterns, we distinguish between the coastal region, where nutrients are upwelled into the euphotic layers, and the offshore region, where subduction by mesoscale eddies dominates (Fig. 1). This separation occurs at a distance of approximately 40 km from the coast, comparable with the width of the continental shelf (Damien et al., 2023). Over the coastal region, the main balance in the NO_3^- budget is between NO_3^- supplied to the euphotic layer by vertical advection and uptake by phytoplankton (Fig. 2). Offshore, horizontal transport (T_h) replaces vertical advection as the main source of NO_3^-. Vertical mixing is also significant offshore, accounting for 33% of the NO_3^- inputs.

In the NO_3^- balance, eddy reaction rates generally oppose mean reaction rates: eddy J^{Uptk} is positive and eddy J^{Nit} is negative. The magnitude of the eddy J^{Uptk} is particularly large, accounting for -$\sim$45% of the mean rate in both the coastal and offshore regions. This eddy contribution is largely dominated by submesoscale.

Near the coast, mean upwelling T_v is the largest source of NO_3^-, and is largely offset (-64%) by submesoscale subduction. The total horizontal advection is negligible, reflecting a balance between the mean T_h, which supply NO_3^-, and eddy T_h, which remove it. The picture is different offshore. Both mean and eddy currents supply NO_3^- at similar rates. NO_3^- delivery by the mean transport is equivalent to that in the coastal region, accounting for 64% of the horizontal NO_3^- supply, while mesoscale and submesoscale components account for 26% and 10% respectively. Along the vertical direction, we observe a close balance between subduction at mesoscales and supply at submesoscales. The magnitude of NO_3^- supply by vertical mixing is similar in both regions ($\sim$ 1.0 10^{-5} mmol m^{-2} s^{-1}), but its relative contribution is more significant offshore (33% of the total NO_3^- supply). This mixing term is largely driven by deepening of the mixed layer in winter (not shown).

The mean J^{Uptk} and its submesoscale rectification show a large seasonal cycle, with a maximum during upwelling in summer (Fig. 3a,b). J^{Nit} follows a similar seasonal cycle, with a maximum following the peak in biological uptake, and is dominated by the mean component (Fig. 3c,d). In contrast, mesoscale eddy reactions show weak seasonality, and large fluctuations on time scales of weeks, especially in summer.

Over the course of the year, the vertical transport near the coast is shaped by mean upwelling (Fig. 3e), and balanced by submesoscale subduction. While mesoscale fluctuations cancel out when integrated over the annual cycle (Fig. 2), they drive the total transport at weekly timescales. Offshore, seasonal variability is less pronounced, and the period of maximum transport follows the upwelling season. Subduction by mesoscale eddies is larger from June to November, when re-supply by submesoscale eddies also increases.

The mean horizontal transport remains small relative to the mesoscale component, which dominates on weekly timescales. Over the year, the horizontal NO_3^- flux from the coast to the open-ocean (Fig. 3 i) is largely positive ($\sim$ 8.3 10^3 molN s^{-1}). This redistribution of nutrients occurs at all scales, with a major contribution from the mean circulation (56%), reflecting wind-driven Ekman transport, followed by mesoscale eddies

(37%). The strong correlation between T_h offshore (Fig. 3 h) and the cross-shore flux (Fig. 3 i) indicates that NO_3^- variations in the open-ocean section of the CCS are mostly caused by transport from the region of active upwelling near the coast (Damien et al., 2023).

4 Discussion and conclusions

4.1 Eddy transport

In the CCS, similar to other EBUS, nutrient subduction by eddies, or "quenching", plays a major role in modulating primary production (Gruber et al., 2011; Nagai et al., 2015; Renault et al., 2016). Here, we show that eddy quenching reflects two contrasting regimes: subduction of freshly-upwelled nutrients by submesoscale eddies nearshore, and by mesoscale eddies further offshore (Figs. 1 and 2). Mesoscale eddies thus transport nutrient from the coast to the open-ocean, but also tend to "bury" them below the euphotic zone (Gruber et al., 2011). Offshore, we observe a near compensation between subduction at mesoscale and delivery at submesoscale (Fig. 2). This balance is particularly evident between July and October, following the large coastal nutrient injection caused by upwelling (Fig. 3). As recently-upwelled nutrients travel offshore and progressively sink along isopycnals, submesoscale eddies tend to resupply them back to the euphotic layer (F. Kessouri et al., 2020).

Globally, submesoscale eddies have been shown to enhance both nutrient delivery to the surface, in particular in the open ocean (Lévy et al., 2001; Mahadevan, 2016), and nutrient and organic matter subduction in regions of strong frontal activity (Omand et al., 2015; Haëck et al., 2023) and upwelling systems (Stukel et al., 2017; F. Kessouri et al., 2020). Here we show that both effects coexist along a gradient of surface nutrient concentrations in the CCS. Specifically, the direction of submesoscale nutrient transport depends on the balance between biological uptake and typical nutrient supply from below the euphotic layer. Relatively long nutrient residence times in surface layers associated with large nutrient concentrations and weak vertical gradients (as observed in nutrient-rich systems) favor nutrient removal by submesoscale currents. In contrast, short surface nutrient residence times associated with low nutrient concentrations and sharp nutriclines (typical of oligotrophic systems) favor submesoscale nutrient supply. This idea is supported by idealized (Freilich et al., 2022) and realistic (F. Kessouri et al., 2020) modelling studies.

4.2 Eddy Reactions

In the California Current, eddies reduce the mean nutrient uptake, and thus net primary production, by about 50%. Most of this compensation (35%) occurs at submesoscale. This eddy rectification is significantly larger than suggested by previous studies, which mostly focused on open-ocean regions and mesoscale circulations (Levy & Martin, 2013; Martin et al., 2015). Our study is the first to directly assess the magnitude of eddy reaction rates using a submesoscale-permitting model and a scale-dependent separation of mesoscale and submesoscale (Capet et al., 2008) in a region with particularly vigorous eddies. At coarser resolution, eddy kinetic energy is likely damped (Capet et al., 2008), thus leading to an underestimate of eddy heterogeneity and its contribution to biogeochemical rates.

Mesoscales and submesoscales are highly advective regimes that favor the emergence of heterogeneity and variability in tracer fields, which cause an eddy rectification of the mean biogeochemical rates. Integrated over large scales and low frequencies, eddy contributions are consistently reducing the mean uptake (Fig. 1 and 2). The magnitude and sign of this eddy rectification result from the eddy covariance of model state variables and the functional dependencies that describe biogeochemical transformations (Equa-

tion 10, see also Levy and Martin (2013)). Because biogeochemical rates depend on several tracers in complex ways (see Supporting Information T2), eddy reaction rates generally involve contributions from the interaction of multiple tracer pairs.

Analysis of the mesoscale contributions to NO_3^- uptake (fig. 4) shows that the dominant terms arise from the saturating response of uptake at high nutrient concentrations (fig. 4 b-d), and the negative correlation between NO_3^- and phytoplankton (Fig. 4 i,j). Specifically, the negative curvature of the Michaelis-Menten saturation function implies that, in a heterogeneous environment, high-frequency events characterized by large NO_3^- concentrations are not as important in boosting uptake, relative to low-NO_3^- events that are instead more effective at reducing it.

Furthermore, assuming a small Damkohler number (i.e., the ratio of the reaction rate to the high-frequency transport rate), Equation 10 can be re-stated by invoking mean tracer gradients and high frequency fluctuations, here assumed to occur mostly along the vertical direction z:

$$\overline{J^{eddy}} \approx \frac{1}{2} \sum_{i,j} \frac{\partial^2 J}{\partial X_i \partial X_j}\bigg|_{\overline{X_i},\overline{X_j},\ldots} \frac{\partial \overline{X_i}}{\partial z} \frac{\partial \overline{X_j}}{\partial z} \overline{\delta z'^2} \tag{11}$$

with $\delta z'$ a small vertical fluctuation. Because vertical profiles of nutrients and phytoplankton show large and opposite gradients, in particular near the base of the euphotic zone, vertical fluctuations enhance the negative covariance between phytoplankton and NO_3^- (Fig. 4 i), producing a sub-surface maximum in the eddy uptake rectification terms.

In contrast, the smaller amplitude of J^{Uptk} rectification at the mesoscale likely reflects a larger influence of horizontal rather than vertical fluctuations, where negative correlations between nutrients and phytoplankton are more ambiguous. Furthermore, this argument is based on a small Damkohler number approximation. Considering a time scale of the order of 1.0 d^{-1} for nutrient uptake (see Supporting Information T2), this approximation is more appropriate for submesoscale rather than mesoscale fluctuations.

When integrated over a full seasonal cycle, we obtain ratios between eddy and mean uptake rates that are remarkably constant ($\sim$ -0.35 for submesoscale and $\sim$ -0.10 for mesoscale) across the CCS. To what extent these ratios can be generalized to different regions and circulation regimes remains an open question.

4.3 Implications

We found a remarkable compensation between mean and submesoscale terms in the net balance of NO_3^- over a seasonal cycle in the California Current System (Fig. 2). This suggests that, in the productive coastal region, nitrate supply occurs predominately at large scales and low frequencies, while removal occurs at small scales and high frequencies. This balance is reversed offshore. While mesoscale contributions tend to cancel out over the seasonal cycle, they generate large variability, producing extremes in both nutrient transport fluxes and uptake rates (Fig. 3 and 4).

The nutrient heterogeneity caused by eddies does not necessarily promote biological productivity. Indeed, it systematically reduces it when averaged over large scales and low frequencies, thus representing a different kind of productivity "quenching" associated with non-linear ecosystem dynamics. The reasons are twofold. First, phytoplankton uptake quickly saturates at high nutrient concentrations. Second, high nutrient concentrations are often associated with low phytoplankton biomass, which limits the potential for increased productivity. We also note that changes in productivity caused by correlations involving temperature (which modulates uptake rates with an exponential dependence) are negligible in the open ocean, but become more important along the continental margin (Fig. 4 g, m, and p).

More generally, we find that eddy terms are far from negligible compared to mean biogeochemical rates. This result questions the ability of coarser models to adequately represent nutrient fluxes and biogeochemical transformations. For example, a non eddy-resolving global model would likely overestimate the vertical nutrient supply and biological uptake along upwelling systems. Physical parameterizations of eddy transport (Gent & McWilliams, 1990; Fox-Kemper et al., 2008) can partially alleviate this issue. However, analogous parameterizations for eddy biogeochemical rates are in early stages of development (Wallhead et al., 2013) and are not yet applied to biogeochemical models. Historically, biases in ocean circulation have been addressed by tuning biogeochemical parameters, which thus implicitly depend not only on the choice of model equations, but also on the resolution at which models are run and evaluated against observations. Our finding of a constant ratio between eddy and mean nutrient uptake rates across a range of circulations ($\sim$ -0.35 for submesoscale and $\sim$ -0.10 for mesoscale), and our analysis of the different contributions of tracer covariance terms to eddy rates, offer new insights for the development of eddy parameterizations of biogeochemical transformations.

Finally, we focused on biological nutrient uptake as the dominant biogeochemical transformation in the highly productive CCS. However, the dynamics of pelagic ecosystems is characterized by many non-linear processes, from food web interactions, to remineralization and microbial dynamics under low oxygen conditions, which remain untouched here. In environments naturally sensitive to multiple stressors, such ocean acidification, warming, and oxygen loss, eddy rectification of ecological processes could greatly alter ecosystem dynamics and marine habitats. Analysis of these processes requires a shift in emphasis from nutrients to carbon and oxygen balances, and from biogeochemical to ecological interactions.

Data Availability Statement

The model code used to generate the simulation is openly available in Kessouri et al. (2020) (`https://doi.org/10.5281/zenodo.398861`). The simulations are reproducible using the setup and forcing described in Damien et al. (2023).

Acknowledgments

This work was supported by NSF grants OCE-1847687 and OCE-1419323, NOAA grants NA15NOS4780186 and NA18NOS4780174, and California Ocean Protection Council grants C0100400 and C0831014. This work used the Expanse system at the San Diego Supercomputer Center through allocation TG-OCE170017 from the Advanced Cyber infrastructure Coordination Ecosystem: Services and Support (ACCESS) program, which is supported by National Science Foundation grants 2138259, 2138286, 2138307, 2137603, and 2138296.

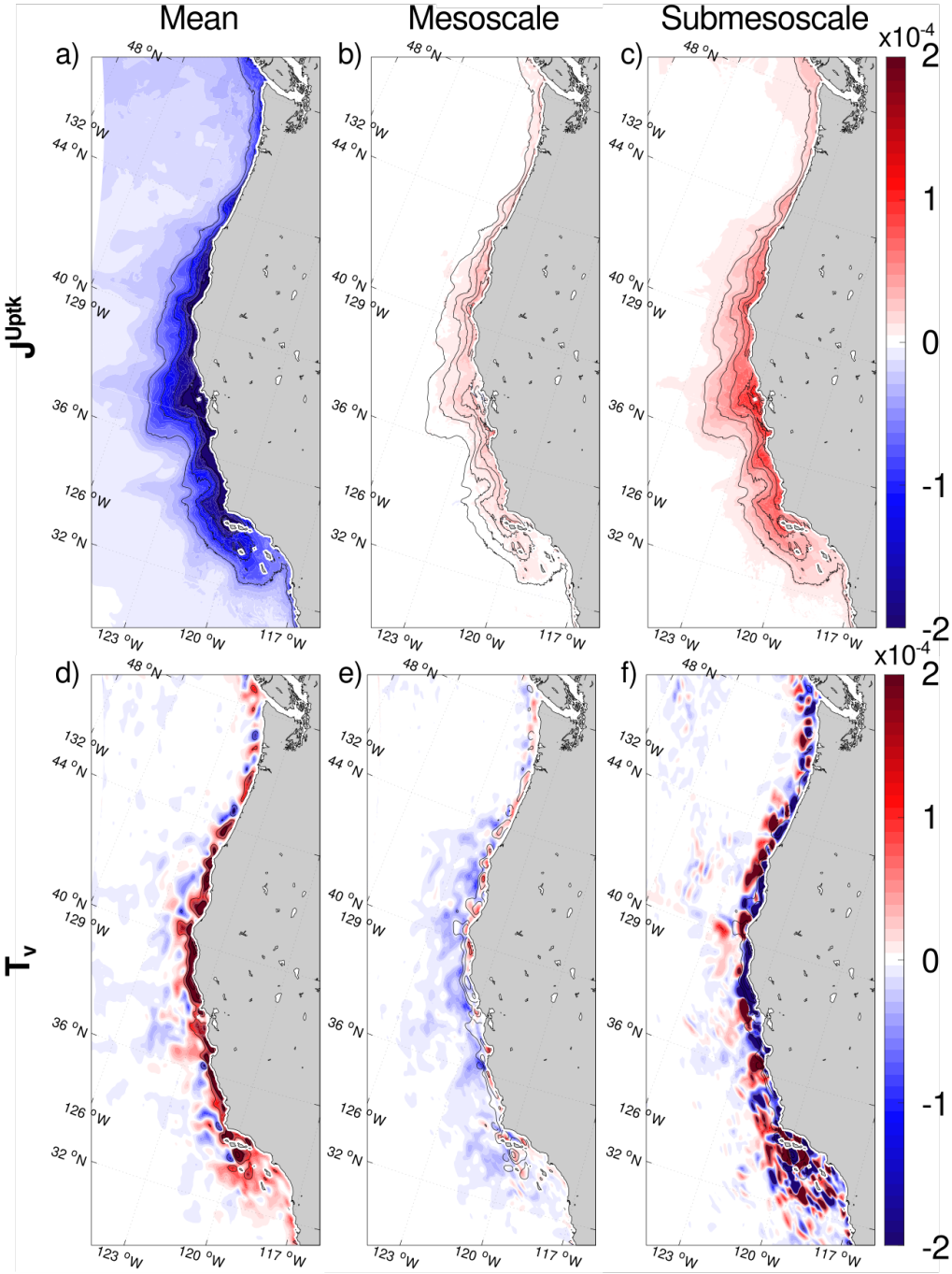

Figure 1. Triple scale decomposition (mean, mesoscale and submesoscale) of (a-c) NO_3^- biological uptake (J^{Uptk}), and (d-f) NO_3^- vertical transport divergence (T_v, equal to the flux at the base of the layer) averaged over a full seasonal cycle and integrated over the euphotic layer ($\sim$ 0-50 m depth). Units are mmol N m^{-2}s^{-1}. Black lines highlight the mean J^{Uptk} isolines of -0.5, -1, -1.5, -2, and -2.5 in the upper panels and the mean T_v isolines of 1, 2 and 5 in the lower panels. A companion figure showing the other terms of the NO_3^- balance is provided in the Supporting Information, Fig. S5, S6.

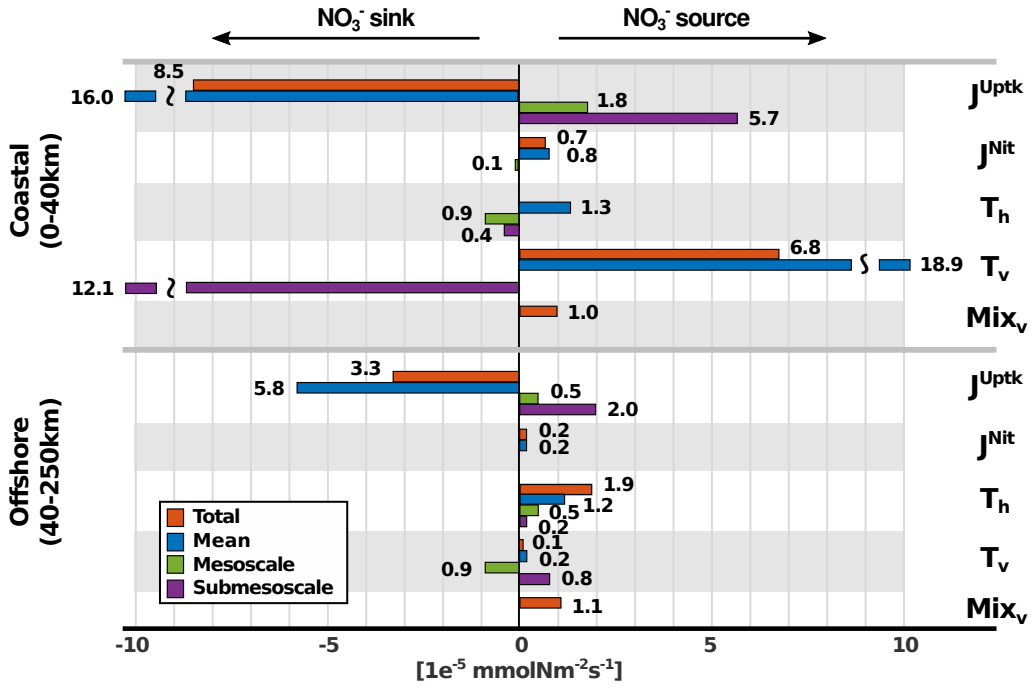

Figure 2. Separation into mean, mesoscale and submesoscale components of the NO_3^- balance terms (Equation 1) integrated in time over a seasonal cycle, in depth over the euphotic layer, and in space over two distinct regions of the U.S. West Coast: a coastal region, from Point Concepcion to Cape Blanco, up to 40km from the coast, and an offshore region up to 250km from the coast. Terms representing negligible component of the fluxes are omitted. Summed up by scales, the NO_3^- balance represents +5.0, +0.8, and -6.8 at respectively mean, mesoscale, and submesoscale in the coastal region, and -4.2, +0.1, and +3.0 offshore. The total adds to 0 when the vertical mixing is included.

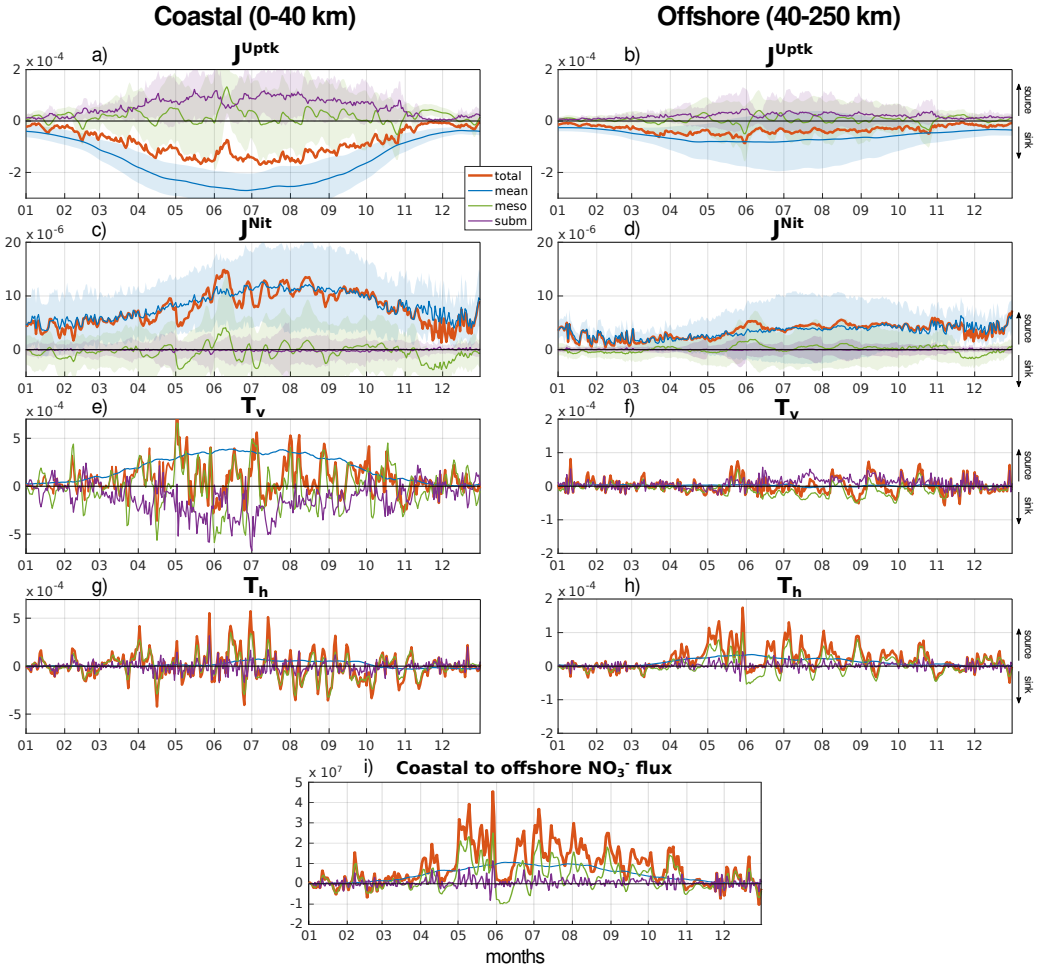

Figure 3. Daily averaged time-series of the (blue) mean, (green) mesoscale, and (purple) submesoscale terms of the NO_3^- balance integrated over the (left panels) coastal and (right panels) offshore regions. In each panel, the red line shows the total rate (calculated online), which equals to the sum of the 3 components. Units are mmol N m^{-2} s^{-1}. The light shaded area shows the +/- standard deviation over the region. This is not included for the transport divergence because it is an order of magnitude larger than the regional average. Note that the y-axis of the transport divergence use a different scale on the left and right panels. Panel (i) shows the time series of the horizontal NO_3^- flux from the coastal to offshore region in mmol N s^{-1}.

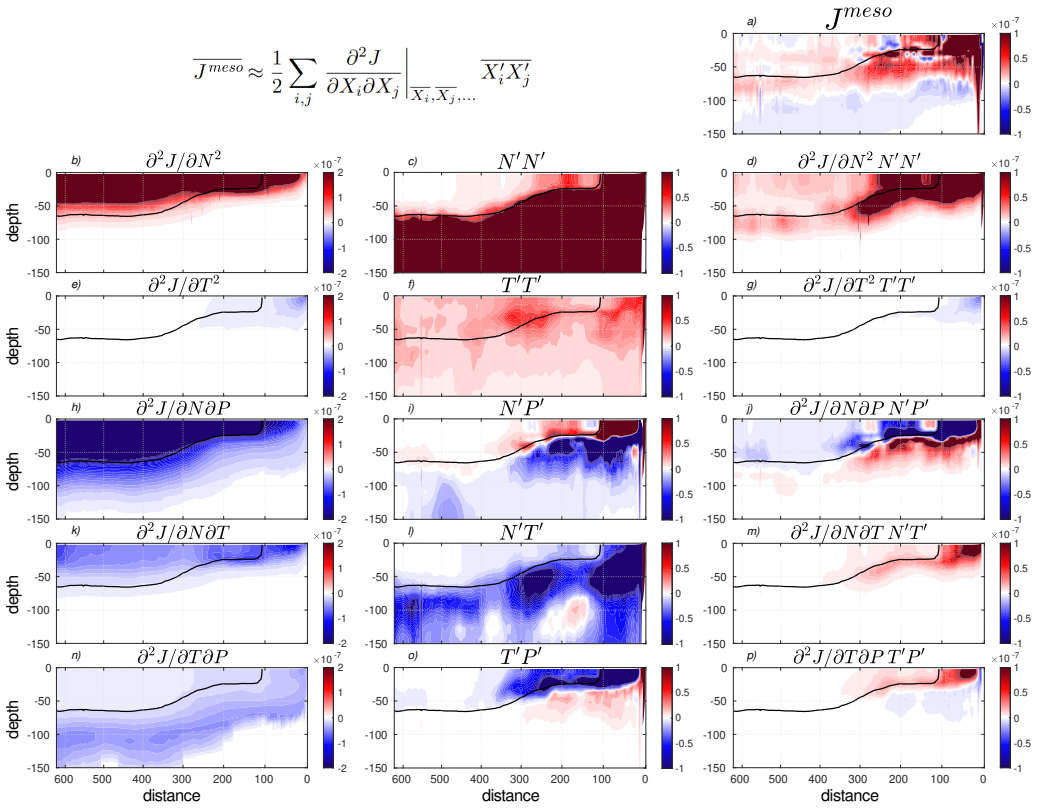

Figure 4. Cross sections, as a function of the distance from the coast and depth, of (a) the annual mean mesoscale eddy uptake, (b,e,h,k,n) the second derivative terms that modulate the (c) nutrient and (f) temperature eddy variance, (i) nutrient-phytoplankton eddy covariance, (l) nutrient-temperature eddy covariance, and (o) temperature-biomass eddy covariance at mesoscale. Following the Taylor series expansion (Equation 10, also shown at the top), the (a) mesoscale eddy uptake is approximated by the sum of the (d,g,j,m,p) second-order terms. Units of the uptake rate are mmol N m^{-3} s^{-1}. The thick black contour represents the nutricline, defined by a nitrate concentration of 1 mmol N m^{-3}. A companion figure comparing eddy covariance at mesoscale and submesoscale is provided in the Supporting Information, Fig. S3.

References

Benitez-Nelson, C. R., Bidigare, R. R., Dickey, T. D., Landry, M. R., Leonard, C. L., Brown, S. L., ... others (2007). Mesoscale eddies drive increased silica export in the subtropical pacific ocean. *Science*, *316*(5827), 1017–1021.

Brentnall, S. J., Richards, K. J., Brindley, J., & Murphy, E. (2003). Plankton patchiness and its effect on larger-scale productivity. *J. of Plankton Res.*, *25*(2), 121–140.

Capet, X., McWilliams, J. C., Molemaker, M. J., & Shchepetkin, A. (2008). Mesoscale to submesoscale transition in the California Current System. part i: Flow structure, eddy flux, and observational tests. *J. Phys. Oceanogr.*, *38*, 29–43.

Carr, M.-E., & Kearns, E. J. (2003). Production regimes in four eastern boundary current systems. *Deep-Sea Res. II: Top. Stud. Oceanogr.*, *50*(22-26), 3199–3221.

Chelton, D. B., Schlax, M. G., Samelson, R. M., & de Szoeke, R. A. (2007). Global observations of large oceanic eddies. *Geophys. Res. Lett.*, *34*(15).

Damien, P., Bianchi, D., McWilliams, J. C., Kessouri, F., Deutsch, C., Chen, R., & Renault, L. (2023). Enhanced biogeochemical cycling along the us west coast shelf. *Global Biogeochem. Cycles*, *37*(1), e2022GB007572.

Deutsch, C., Frenzel, H., McWilliams, J. C., Renault, L., Kessouri, F., Howard, E., ... Yang, S. (2021). Biogeochemical variability in the california current system. *Progr. Oceanogr.*, *196*, 102565.

Falkowski, P. G., Ziemann, D., Kolber, Z., & Bienfang, P. K. (1991). Role of eddy pumping in enhancing primary production in the ocean. *Nature*, *352*(6330), 55–58.

Fox-Kemper, B., Ferrari, R., & Hallberg, R. (2008). Parameterization of mixed layer eddies. part i: Theory and diagnosis. *J. Phys. Oceanogr.*, *38*(6), 1145–1165.

Freilich, M. A., Flierl, G., & Mahadevan, A. (2022). Diversity of growth rates maximizes phytoplankton productivity in an eddying ocean. *Geophys. Res. Lett.*, *49*(3), e2021GL096180.

Frenger, I., Bianchi, D., Stührenberg, C., Oschlies, A., Dunne, J., Deutsch, C., ... Schütte, F. (2018). Biogeochemical role of subsurface coherent eddies in the ocean: Tracer cannonballs, hypoxic storms, and microbial stewpots? *Global Biogeochem. Cycles*, *32*(2), 226–249.

Gaube, P., McGillicuddy Jr, D. J., Chelton, D. B., Behrenfeld, M. J., & Strutton, P. G. (2014). Regional variations in the influence of mesoscale eddies on near-surface chlorophyll. *J. Geophys. Res. Oceans*, *119*(12), 8195–8220.

Gent, P. R., & McWilliams, J. C. (1990). Isopycnal mixing in ocean circulation models. *J. Phys. Oceanogr.*, *20*(1), 150–155.

Goodman, L. (2011). Application of the robinson biodynamical theory to turbulence. *Dyn. atmospheres oceans*, *52*(1-2), 8–19.

Goodman, L., & Robinson, A. R. (2008). On the theory of advective effects on biological dynamics in the sea. iii. the role of turbulence in biological–physical interactions. *Proc. R. Soc. A: Math. Phys. Eng. Sci.*, *464*(2091), 555–572.

Gruber, N., Lachkar, Z., Frenzel, H., Marchesiello, P., Münnich, M., McWilliams, J., ... Plattner, G. (2011). Eddy-induced reduction of biological production in eastern boundary upwelling systems. *Nat. Geosci.*, *4*, 787–792.

Haëck, C., Lévy, M., Mangolte, I., & Bopp, L. (2023). Satellite data reveal earlier and stronger phytoplankton blooms over fronts in the gulf stream region. *Biogeosciences*, *20*(9), 1741–1758. Retrieved from `https://bg.copernicus.org/articles/20/1741/2023/` doi: 10.5194/bg-20-1741-2023

Kessouri, McWilliams, C. J., Deutsch, C., Renault, L., Frenzel, H., Bianchi, D., & Molemaker, J. (2020). *Roms-bec oceanic physical and biogeochemical model code for the southern california current system v2020.* Zenodo. Retrieved from `https://doi.org/10.5281/zenodo.3988618` doi: 10.5281/zenodo.3988618

Kessouri, F., Bianchi, D., Renault, L., McWilliams, J., Frenzel, H., & Deutsch, C. (2020). Submesoscale currents modulate the seasonal cycle of nutrients and productivity in the california current system. *Global Biogeochem. Cycles*, *34*(10), e2020GB006578.

Lathuilière, C., Echevin, V., Lévy, M., & Madec, G. (2010). On the role of the mesoscale circulation on an idealized coastal upwelling ecosystem. *J. Geophys. Res. Oceans*, *115*, C09016.

Lévy, M., Ferrari, R., Franks, P. J., Martin, A. P., & Rivière, P. (2012). Bringing physics to life at the submesoscale. *Geophys. Res. Lett.*, *39*(14).

Lévy, M., Franks, P. J., & Smith, K. S. (2018). The role of submesoscale currents in structuring marine ecosystems. *Nat. Commun.*, *9*(1), 1–16.

Lévy, M., Klein, P., & Treguier, A.-M. (2001). Impact of sub-mesoscale physics on production and subduction of phytoplankton in an oligotrophic regime. *J. Mar. Res.*, *59*(4), 535–565.

Levy, M., & Martin, A. (2013). The influence of mesoscale and submesoscale heterogeneity on ocean biogeochemical reactions. *Global Biogeochem. Cycles*, *27*(4), 1139–1150.

Lovecchio, E., Gruber, N., & Münnich, M. (2018). Mesoscale contribution to the long-range offshore transport of organic carbon from the Canary Upwelling System to the open North Atlantic. *Biogeosciences*, *15*, 5061–5091.

Mahadevan, A. (2016). The impact of submesoscale physics on primary productivity of plankton. *Ann. rev. mar. sci.*, *8*, 161–184.

Marchesiello, P., McWilliams, J. C., & Shchepetkin, A. (2003). Equilibrium structure and dynamics of the California Current System. *J. Phys. Oceanogr.*, *33*, 753–783.

Martin, A. P., Lévy, M., Van Gennip, S., Pardo, S., Srokosz, M., Allen, J., ... Pidcock, R. (2015). An observational assessment of the influence of mesoscale and submesoscale heterogeneity on ocean biogeochemical reactions. *Global Biogeochem. Cycles*, *29*(9), 1421–1438.

McGillicuddy, D. (2016). Mechanisms of physical-biological-biogeochemical interaction at the oceanic mesoscale. *Ann. Rev. Mar. Sci.*, *8*, 125–159.

McGillicuddy, D., Anderson, L., Doney, S., & Maltrud, M. (2003). Eddy-driven sources and sinks of nutrients in the upper ocean: Results from a 0.1 resolution model of the north atlantic. *Global Biogeochem. Cycles*, *17*(2).

Messié, M., Ledesma, J., Kolber, D. D., Michisaki, R. P., Foley, D. G., & Chavez, F. P. (2009). Potential new production estimates in four eastern boundary upwelling ecosystems. *Progr. Oceanogr.*, *83*, 151–158.

Moore, J. K., Doney, S. C., & Lindsay, K. (2004). Upper ocean ecosystem dynamics and iron cycling in a global three-dimensional model. *Global Biogeochem. Cycles*, *18*.

Nagai, T., Gruber, N., Frenzel, H., Lachkar, Z., McWilliams, J. C., & Plattner, G.-K. (2015). Dominant role of eddies and filaments in the offshore transport of carbon and nutrients in the California Current System. *J. Geophys. Res. Oceans*, *120*, 5318–5341.

Omand, M. M., D'Asaro, E. A., Lee, C. M., Perry, M. J., Briggs, N., Cetinić, I., & Mahadevan, A. (2015). Eddy-driven subduction exports particulate organic carbon from the spring bloom. *Science*, *348*(6231), 222–225.

Oschlies, A., & Garcon, V. (1998). Eddy-induced enhancement of primary production in a model of the north atlantic ocean. *Nature*, *394*(6690), 266–269.

Renault, L., Deutsch, C., McWilliams, J. C., Frenzel, H., Liang, J.-H., & Colas, F. (2016). Partial decoupling of primary productivity from upwelling in the california current system. *Nature Geosci.*, *9*, 505–508.

Renault, L., McWilliams, J. C., Jousse, A., Deutsch, C., Frenzel, H., Kessouri, F., & Chen, R. (2021). The physical structure and behavior of the california current system. *Progr. Oceanogr.*, *195*, 102564.

Rovinsky, A. B., Adiwidjaja, H., Yakhnin, V. Z., & Menzinger, M. (1997). Patchiness and enhancement of productivity in plankton ecosystems due to the differential advection of predator and prey. *Oikos*, 101–106.

Shchepetkin, A. F., & McWilliams, J. C. (2005). The Regional Oceanic Modeling System (ROMS): a split-explicit, free-surface, topography-following-coordinate oceanic model. *Ocean Model.*, *9*, 347–404.

Stukel, M. R., Aluwihare, L. I., Barbeau, K. A., Chekalyuk, A. M., Goericke, R., Miller, A. J., ... others (2017). Mesoscale ocean fronts enhance carbon export due to gravitational sinking and subduction. *Proc. Natl. Acad. Sci. U.S.A.*, *114*(6), 1252–1257.

Wallhead, P. J., Garçon, V. C., & Martin, A. P. (2013). Efficient upscaling of ocean biogeochemistry. *Ocean Model.*, *63*, 40–55.

Wallhead, P. J., Martin, A. P., & Srokosz, M. A. (2008). Spatially implicit plankton population models: transient spatial variability. *J. Theor. Biol.*, *253*(3), 405–423.

Yamamoto, A., Palter, J. B., Dufour, C. O., Griffies, S. M., Bianchi, D., Claret, M., ... Galbraith, E. D. (2018). Roles of the ocean mesoscale in the horizontal supply of mass, heat, carbon, and nutrients to the northern hemisphere subtropical gyres. *J. Geophys. Res. Oceans*, *123*(10), 7016–7036.